LEGENDS TO SUPPLEMENTARY FIGURES

SUPPLEMENTARY FIGURE S1. Distribution of human genomic compositional features vs. time of replication. Shown are distributions vs. replication time of G+C and CpG putatively neutral sites; and densities of annotated exons (RefSeq), genes (RefSeq), conserved non-coding sequences (CNS)[25], and recombination hotspots[24].

SUPPLEMENTARY FIGURE S2. Linear regression analysis of the partial model controlling for all predictors except replication time. Shown are partial residual (**A**) and partial regression (**B**) plots of partial regression model with the replication time predictor removed, fitted to human-chimpanzee divergence (**top row**), human-macaque divergence (**middle row**), and human SNP density (**bottom row**), non-CpG neutral sites. See **Supplemental Table S2** for full regression model parameters. Lines on plots represent linear fit of residuals vs. replication state component. In all cases, the fitted lines demonstrate similar linear increasing trend indicating significant and consistent contribution of replication time to response (mutation rate) when simultaneously controlling for all other predictors in the model.

SUPPLEMENTARY FIGURE S3. Comparison of performance of different window sizes for sampling divergence and SNP density. Shown is dependence of human-chimpanzee divergence (**A**), human-macaque divergence (**B**), and human SNP density (**C**) on time of replication in putatively neutral non-CpG sites. Non-overlapping windows of 30kb, 50kb, and 100kb in size were tested in each case and revealed identical trends. Larger windows were not utilized due to the high resolution of the replication timing partitioning data (average segment size <75kb). Both 30kb and 50kb windows

demonstrate similar performance but the former showed high levels of sampling errors when utilized for more sparse datasets (data not shown), while the use of 100kb window size result in inflated variance and decreased resolution.

SUPPLEMENTARY FIGURE S4. Dependence of human-chimpanzee divergence on time of DNA replication at different classes of sites. Shown is dependence of human-chimpanzee divergence on time of replication in non-CpG sites annotated as ancestral repeats (**A**), coding 4-fold degenerate (**B**), conserved non-coding (**C**), and coding non-degenerate (**D**). The first two examples represent sites under relaxed selection while the latter two are assumed to be under strong selective pressure. In all cases, the same increasing trend is observed, with S4/S1 gain in substitution rates of 20%, 81%, 38%, and 176% for the four types of sites, respectively. Note: Results for coding 4-fold degenerate sites are unreliable due to the low frequency of mutations detected (total number of such substitutions = 196).

SUPPLEMENTARY FIGURE S5. Dependence of lineage-specific divergence on time of DNA replication. Shown is a comparison between dependence of human-chimpanzee divergence on time of replication in the human lineage (**A**) and in the chimpanzee lineage (**B**). A three-way human-chimpanzee-macaque alignment was used to polarize and analyze separately substitutions in the human and chimpanzee lineages. Non-parsimonious substitutions were discarded and only non-CpG putatively neutral sites were utilized (see **Fig. 1**). The increase in substitution rate between S4/S1 temporal replication states equals 23% in the case of both human and chimpanzee lineages ($p < 3.75 \times 10^{-18}$).

SUPPLEMENTARY FIGURE S6. Replication time-dependence of divergence and SNP density genome-wide. Shown are Human-chimpanzee divergence (left column), human-macaque

divergence (middle column), and human SNP density (right column) computed for all putatively neutral sites (**A-C**), non-CpG neutral sites (**D-F**), and neutral CpG sites (**G-I**) using genome-wide replication timing (early vs. late) data[14]. For the purpose of the analysis, 20% of the lowest scoring (ratio < 1.24) and 20% the highest scoring (ratio > 1.66) segments from 1Mb human genome dataset[14] were selected and designated as S4 (late replicating) and S1 (early replicating), correspondingly. The fraction of sites in each was calculated as described in **Fig. 1** but with the nucleotide counts pooled without window sampling. The estimated increase in mutation rates between the S1 and S4 temporal replication states (see panel legends) was highly significant at $p < 2.2 \times 10^{-16}$ (χ^2 test) in all cases.

SUPPLEMENTARY FIGURE S7. Replication time distribution of pooled transitions, pooled transversions, and individual mutation types in putatively neutral sites. For human-chimpanzee (**A**) and human-macaque (**B**) divergence, shown are distributions vs. replication time of pooled transitions, pooled transversions, and transvertions that can be enumerated individually.

SUPPLEMENTARY FIGURE S1

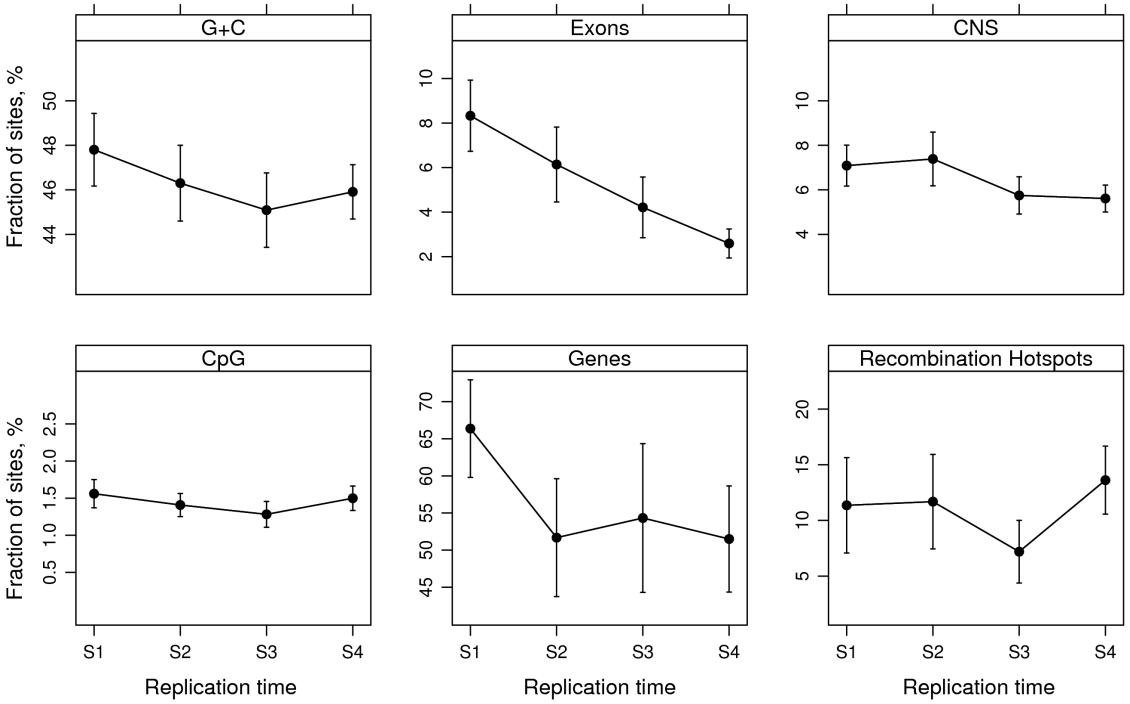

SUPPLEMENTARY FIGURE S2

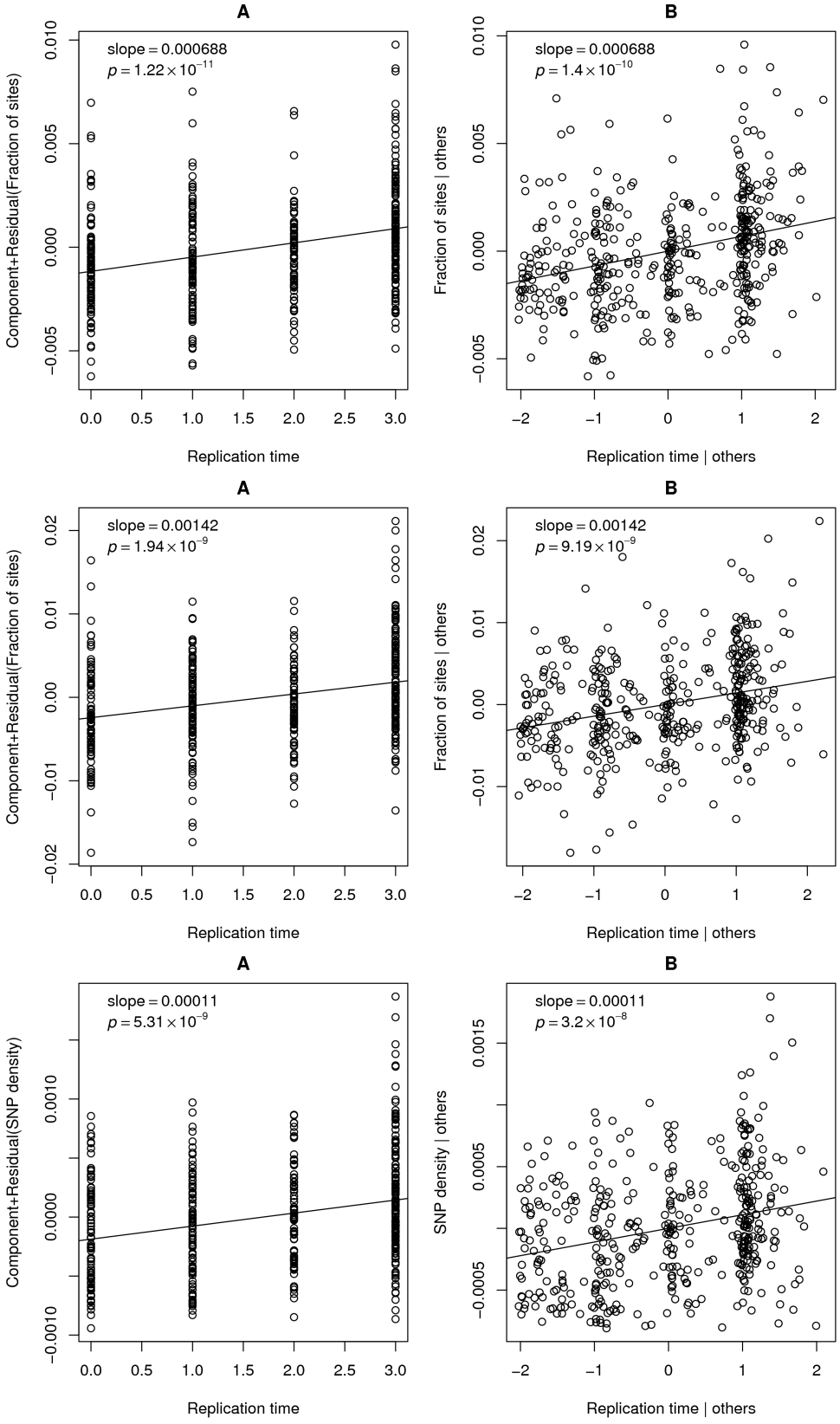

SUPPLEMENTARY FIGURE S3

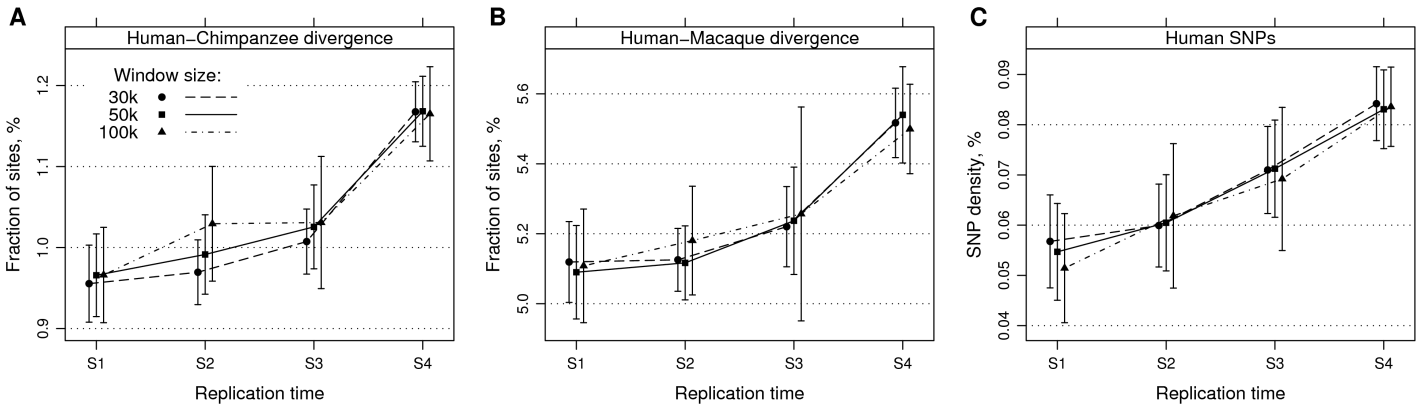

SUPPLEMENTARY FIGURE S4

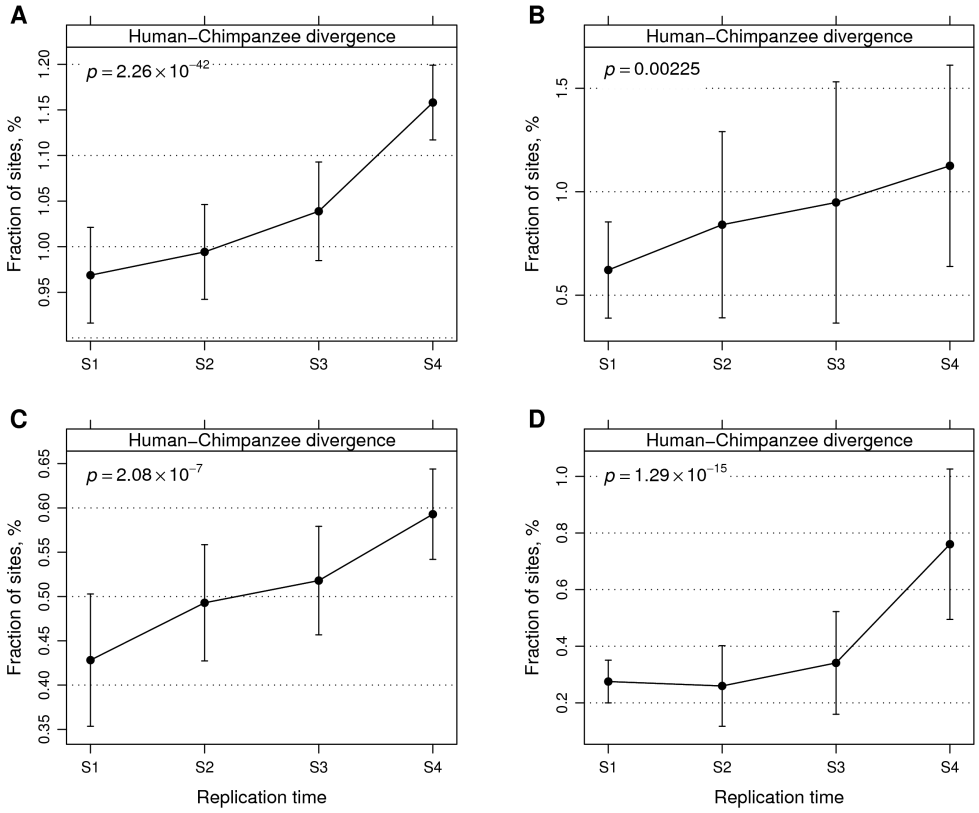

SUPPLEMENTARY FIGURE S5

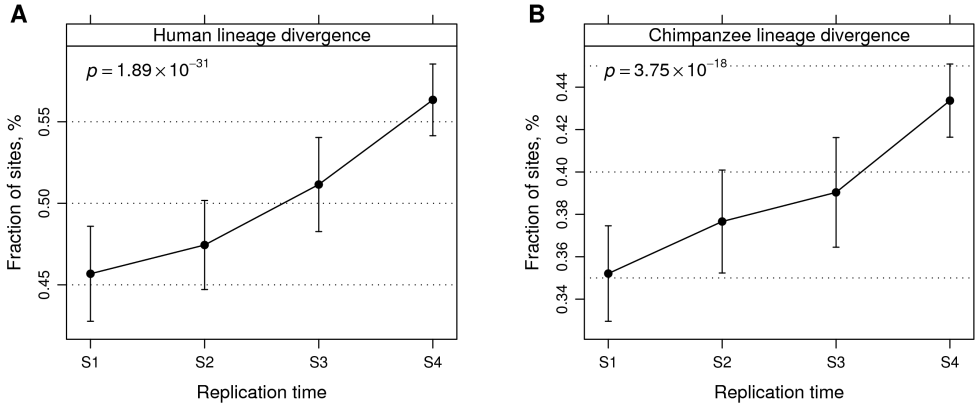

SUPPLEMENTAL FIGURE S6

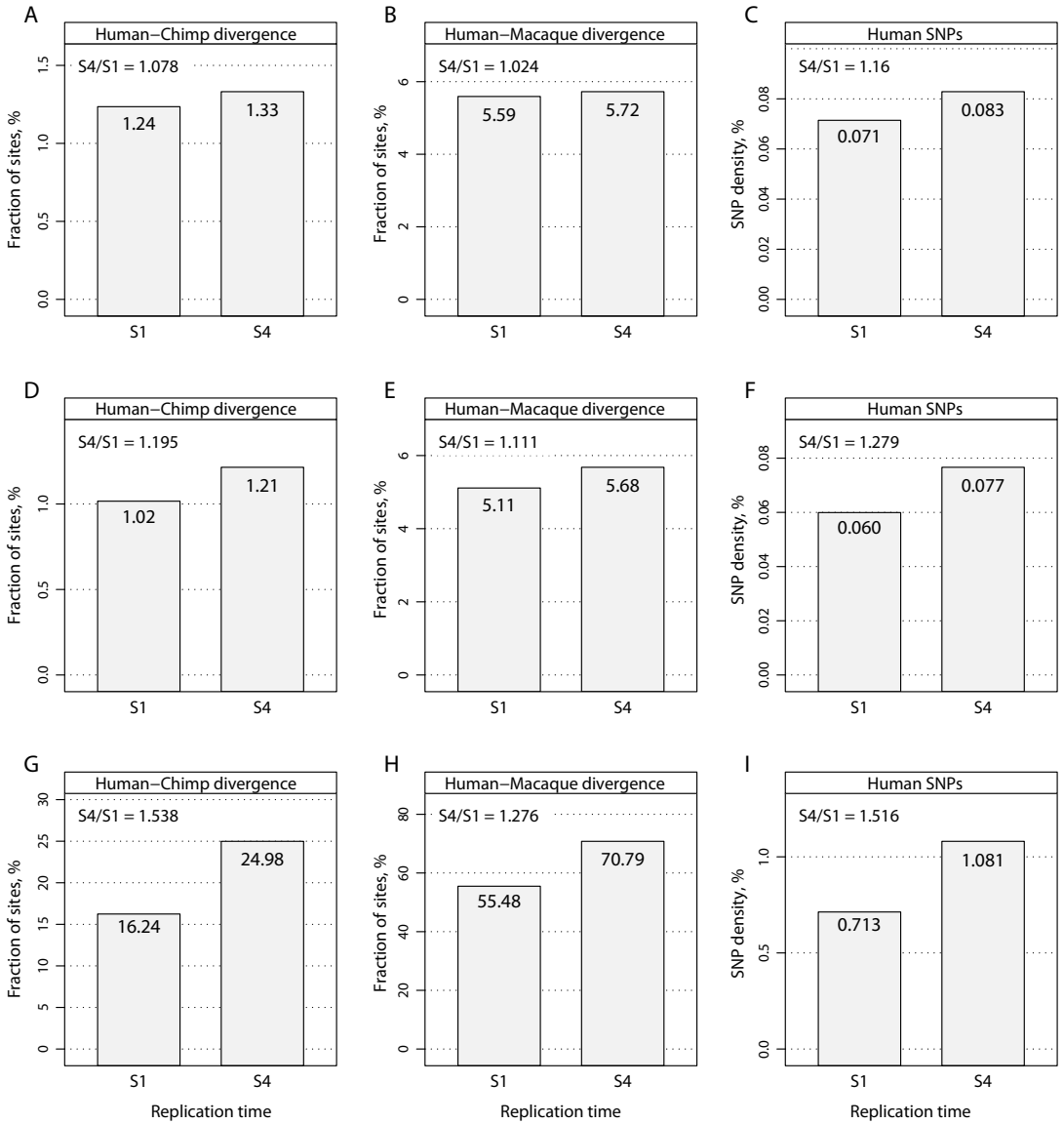

SUPPLEMENTARY FIGURE S7